Appl. Phys. A 42, 1–18 (1987)

Applied Physics A Solids and Surfaces

Photoluminescence of Transition Metal Complexes in Silicon

H. Conzelmann*

Physikalisches Institut, Teil 4, Universität, Pfaffenwaldring 57, D-7000 Stuttgart, Fed. Rep. Germany

Received 8 July 1986/Accepted 1 August 1986

Abstract. Results of luminescence studies on silicon doped with the 3*d* transition metals are reviewed. Spectra are observed after V, Cr, Mn, Fe, and Cu diffusion. We discuss the problems of center identifications, using the example of the CrB-pair luminescence. Level schemes for the optical transitions are discussed and correlated with electrical level positions of TM defects. Luminescent centers can be divided into two classes: CrB, CrGa, and Mn_4 are effective recombination centers with low quantum efficiencies, whereas Fe and Cu associated spectra show characteristics of exciton decay at isoelectronic centers, e.g. show a high quantum efficiency. The phonon structure of the spectra is discussed, and it is shown that the local mode energies of the centers follow a systematic trend.

PACS: 71.55; 78.55; 71.35

Transition metals (TM) are dreaded contaminations in silicon, since they influence its electronic properties even in very low concentrations [1–3] and because they are easily introduced due to their high diffusivity [4, 5]. TM-correlated defects give rise to a manifold of deep levels within the band gap [5–11] and often act as very efficient recombination centers [1–3, 12, 13]. Therefore it has been the aim of many investigations to identify TM impurities by various measurement techniques, e.g. Electron Paramagnetic Resonance (EPR) [4, 14, 15], Hall measurements or Deep Level Transient Spectroscopy (DLTS) [5–11], and to characterize the physical properties of the defects.

The first systematic studies were the EPR investigations of Ludwig and Woodbury [14, 15]. They determined the chemical nature and the electronic ground state configuration of the interstitial and substitutional metals and some TM complexes, e.g. interstitial TM – shallow acceptor pairs. A vast number of publications during the last two decades dealt with the electrical levels within the band gap introduced by TM doping [6, 7]. The data were quite confusing and often controversal. It was until very recently when detailed studies, often combining different methods of investigations (DLTS, Hall, EPR, and luminescence), allowed a clear identification of a deep level with a defect of known chemical structure [5, 8–11, 16]. Although there are now confirmed level positions for many of the 3*d*-impurities in Si, there is still a lack of investigations which can give informations beyond these data as about excited TM states and the role the centers play for carrier recombination.

Luminescence measurements are frequently and successfully applied to study impurities in various semiconductors. A prominent example is the deep-donor luminescence of oxygen in GaP [17, 18], where the luminescence data yielded a complete picture of the chemical and electronic structure of the defect. Also TM centers in III/V-semiconductors have been extensively studied [19] by the different luminescence techniques. Spectra recorded under application of uniaxial stress- or magnetic fields to the samples allow us to determine defect symmetries and the quantum numbers of electronic states, from temperature controlled measurements level schemes can be deduced which often may be correlated with the electrical level of a defect and the phononstructure of the luminescence

* Present address: Telefunken electronic GmbH, Theresienstrasse 2, D-7100 Heilbronn, FR Germany

band gives a lot of information about electron lattice coupling.

In silicon, the near-band-gap luminescence of excitons bound to shallow donors or acceptors has been studied in detail since 1960 [20–22]. The spectra – characteristic for the dopant – can be used for a qualitative, sometimes even quantitative analysis of Si, e.g. to determine the level of compensation [23, 24]. However, only few spectra of deep centers and none for an identified TM defect were reported until the end of the 1970 decade. This lack may be due to the usually low quantum efficiency of optical transitions in silicon in connection with the partially low solubility of TM and the previous lack of sensitive detectors for wavelengths above 1.2 μm, needed to observe the deep optical transitions. In 1980, J. Weber and coworkers reported new deep luminescence lines in Si doped with iron [25, 26] and thereafter spectra were observed in silicon intentionally doped with copper [27–29], chromium [16, 30], and manganese [31].

In the present paper, luminescence studies on silicon doped with 3*d*-TM are reviewed. We will show common and distinguishing features of the spectra concerning their electronic level schemes, the phonon structure and the importance of the luminescent defect on free carrier recombination as far as these properties can be determined from luminescence. After a short section on the experimental set up and sample preparation technique we will use the CrB-pair luminescence as an example to demonstrate the problems of defect identification.

1. Experimental

The samples used for our experiments were prepared by diffusing the elemental TM into dislocation- and swirl-free n- and p-type silicon crystals. The concentrations of shallow dopants in the starting materials ranged from 10^{13} to $10^{19}\,cm^{-3}$. Most of the samples were prepared from float-zone refined crystals. Some samples from Czochralski grown materials showed identical results. Contamination with the transition element was achieved mostly by evaporation (Ti, V, Cr, Mn, Fe, and Cu), but also by rubbing metal wire (Ti, V, Fe, Co, and Ni) on the surface of the silicon slices. Cr and Mn were also introduced by ion implantation [32]. For the heat treatments we used two different furnace systems: In one we sealed the samples in evacuated quartz ampoules which were then annealed in a gas stream of oxygen. To keep TM of high diffusivity on interstitial lattice sites, e.g. to prevent the formation of precipitates, it is necessary to minimize the cooling time after the diffusion process [4]. Therefore, after the heat treatment the ampoules were rapidly cooled to room temperature by dropping the whole ampoule into water. The second system was vertically arranged and the samples were diffused in a stream of argon or oxygen. Here the samples could be quenched to room temperature by a mechanism which allows their direct dropping into silicone oil. The cooling rate was about 1000° C/s, whereas in the case of diffusion in ampoules it was around 100° C/s.

The samples were then mechanically and chemically polished to remove the metal alloy from the surface and to increase the surface quality. The samples were stored in liquid nitrogen until they were measured.

For the luminescence measurements, the samples were mounted in a variable temperature cryostat (range from 2 K to around room temperature) in which also uniaxial stress could be applied to sample parallelepipeds of $2 \times 2 \times 7\,mm^3$. Measurements in magnetic fields (Voigt configuration) up to 5.3 T were possible in a He immersion cryostat. For excitation an Ar- or Kr-ion laser was used with a maximum output of 6 W cw. The luminescence light was dispersed with a Spex monochromator (Model 1702). Near band gap luminescence was detected with a photomultiplier with S1 cathode, longer wavelengths with a Ge detector (North Coast type EO-817, up to 1.6 μm) or a PbS detector (Santa Barbara, Type 40742, up to 2.5 μm). The signals were processed in lock in technique.

2. Defect Identification and Characterization Example: The CrB Pair

It is a severe and often unresolvable problem to associate measured defect properties to a well-defined atomistically identified center. The scatter of level positions reported in literature during the last two decades for each of the 3*d*-elements in Si is an impressive example for the difficulties which arise [6, 7]. The identification of a luminescent defect is no less problematical although the energetic resolution is much better than for electrical measurements and different defects can be clearly distinguished by their specific spectra. On the other hand, luminescence gives no a priori information about defect concentrations, which would be helpful for identification by correlating them with those determined by other methods. There are defects with high quantum efficiencies of transitions, so even very low defect concentrations ($<10^{12}\,cm^{-3}$) yield high luminescence intensities, whereas centers with dominating non radiative transitions or low optical transition probabilities are not observable even in concentrations of $10^{17}\,cm^{-3}$.

We want to demonstrate some criteria for defect identification using the example of the CrB-pair luminescence. In this case the identification seems to be assured by many experiments [16, 30]. In following

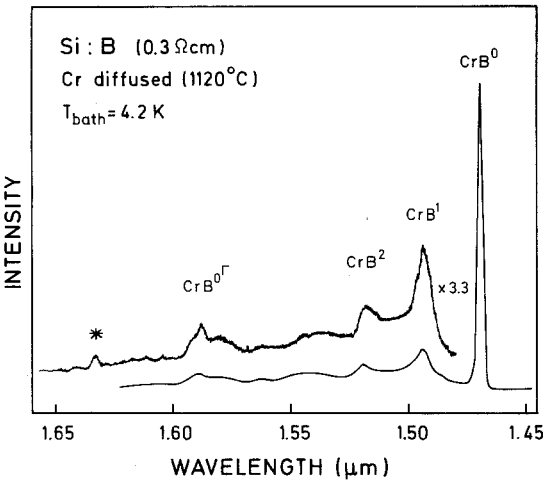

Fig. 1. Spectrum of CrB pairs at a bath temperature of 4.2 K

chapters we will then apply these criteria to the luminescence spectra observed after doping of Si with other 3*d* elements.

The diffusion of chromium into boron doped silicon (1 Ω cm) yields the spectrum (T_{bath} = 4.2 K) shown in Fig. 1. The spectrum consists of a no-phonon (NP) line CrB^0 at 1.479 μm and the structured phonon sideband (CrB^1, CrB^2, and $CrB^{0'}$). These phonon replicas appear at all TM spectra due to a coupling of the transitions to lattice phonons or localized defect vibrations. Since the phonon coupling is of special interest it will be discussed in detail in Sect. 5. The absolute intensity of the spectrum is rather low, two orders of magnitude lower than that one of the boron bound exciton in the starting material.

Two questions arise: Is the spectrum really originating from Cr or form other unintentionally introduced impurities the luminescent defect, and – if it is Cr – how could the specific Cr complex responsible for the luminescence be identified?

First, one has to accept that residual impurities of the order of $10^{12}\,cm^{-3}$ may be always present in the samples. One of those impurities may form a complex with high quantum efficiency which is responsible for the spectrum. To exclude this possibility we prepared control samples running through all steps but not chromium contaminated and – even more significant – we varied the conditions of Cr doping. Samples were therefore diffused in evacuated ampoules or in a stream of argon or oxygen. The samples were chromium plated by evaporation or by ion implantation. Since the different methods should result in variations of residual impurities we believe that the quantitative reproducibility of our luminescence signal in these Si:Cr samples is a strong evidence that the luminescence indeed is originated by chromium.

For some luminescence systems, the defect atoms can be identified by line shifts, which arise when different isotopes of the dopant are used. The energies of local defect vibrations are influenced by the mass of the moving atom, so different isotopes of the same element can be distinguished by small line shifts, especially in the local mode replicas (see also Sect. 5). The intentional doping with different isotopes helped for example to identify the copper luminescence [27] (Sect. 3.5) and some radiation induced defects in silicon associated with C, B, and Li [29, 33–35]. However, for chromium the phonon sideband was too weak and too broad to resolve the small isotopic shifts expected for the different Cr isotopes.

The identification of the chromium complex is now achieved by comparing specific properties of the luminescent defect with those of chromium complexes reported in literature and determined with other methods (EPR, DLTS).

2.1. Variation of Concentrations of Chromium and Shallow Dopants

We have investigated the dependence of the luminescence intensity on type and concentration of the dopant in the starting material used and on the Cr-diffusion temperature (Fig. 2). Since the Cr signals have been found only in boron doped silicon and measurements in uniaxial stress fields have shown that the center has trigonal symmetry [30] in agreement with the ⟨111⟩ axis of the CrB pair [14] an identification of the luminescent center with the CrB pair is suggested. In Fig. 2 (right part) the CrB^0 intensity is plotted against the B concentration at a fixed diffusion temperature of 1200° C corresponding to a Cr concentration

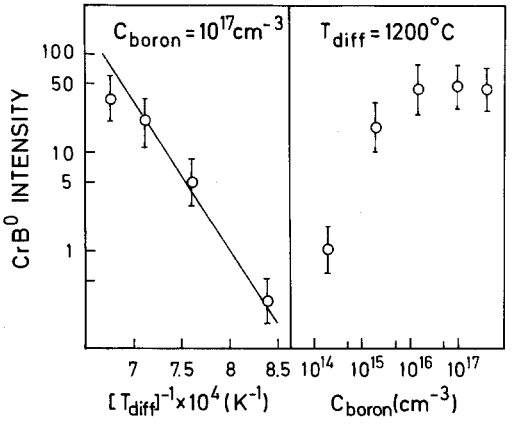

Fig. 2. Left part: The intensity of the CrB^0 line as a function of the inverse diffusion temperature at a fixed boron concentration of $10^{17}\,cm^{-3}$. The straight line follows the solubility of Cr [4]. Right part: The intensity dependence on the B concentration at a constant Cr content ($2 \times 10^{15}\,cm^{-3}$)

of $2\times10^{15}\,cm^{-3}$. The intensity increases with the B concentration until the B content exceeds that of Cr. Then saturation is reached since all Cr atoms are bound in CrB pairs. On the other hand (left part of Fig. 2), the diffusion temperature is varied whereas the B concentration was fixed well above the maximum solubility of chromium in Si ($C_B=10^{17}\,cm^{-3}$), therefore Cr is completely bound in CrB-pairs. The data points follow the temperature dependence of the solubility of Cr, as determined by Weber [4] (straight line in Fig. 2). We conclude that the CrB-luminescence intensity is indeed proportional to the concentration of CrB pairs in the samples.

2.2. *Annealing Experiments*

Annealing experiments can be a helpful tool for center identification when characteristics of the observed anneal out of a signal correspond to those of a known defect. However, often the interpretation of annealing experiments is not straightforward. The specific sample properties, e.g. the defect concentration itself, doping and dopants of the starting material or velocity of quenching after annealing steps determine the possible chemical reactions and the equilibrium concentrations in the solid via the law of mass action. Only for well defined samples and well defined reactions data obtained from different samples are comparable. To exclude these difficulties, identical samples were investigated with different measurement techniques [DLTS, EPR, and luminescence (Lumi)] [16]. The results of isochronal annealing experiments are depicted in Fig. 3, for samples with three different boron concentrations. The solid lines were calculated for the reaction

$$Cr_i^+ + B_s^- \rightarrow CrB^0 \tag{1}$$

with the law of mass action

$$[CrB]/[Cr] = [B]A\exp(U/kT) \tag{2}$$

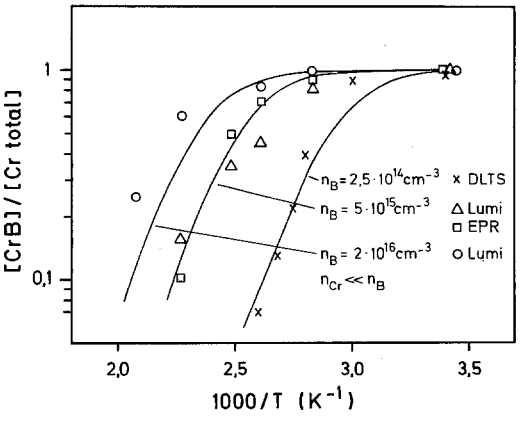

Fig. 3. Isochronal annealing of CrB pairs

and a binding energy $U=0.65\,eV$ ($A\cong10^{-23}\,cm^{-3}$) [16]. The different experimental techniques among each other as well as the calculated anneal are in excellent agreement, thus further supporting the tentative identification. For the highest boron concentration, the stability of the pair is somewhat increased since it is then in the positive charge state forming a more stable $Cr^{2+}B^-$ complex. For a detailed discussion of reactions among various transition metal donors and group III acceptors we refer to [9]. We note that the binding energy for many pairs, e.g. $U\cong0.6\,eV$ for CrB, is roughly in accordance with that one of two point charges of opposite sign on the substitutional and nearest T_d-interstitial site ($U\cong0.55\,eV$). Lemke [9] reported values for U between 0.3 and 0.7 eV for TM-donor-acceptor pairs in their neutral charge state.

2.3. *Level Scheme of the Optical Transitions*

After the successful center identification we can turn to its electronic properties, e.g. we can try to correlate the level scheme of the transitions with electrical levels of the center determined by DLTS or Hall measurements. Sauer and Weber [29] have already mentioned that the luminescence ground state determined from temperature controlled measurements seem to be correlated with the DLTS level position for TM-associated centers. This implies that the observed luminescence initiates at a rather shallow excited state near a band edge and ends in the ground state of the defect in a special charge state. At the moment we will accept this interpretation without proof, but we will discuss this in more detail in Sect. 4.

If the excited state of the defect (initial state of the optical transition) and the carriers in the nearby band are in thermal equilibrium, e.g. the relaxation time constant is much smaller than the lifetime of the excited state, and there is a constant generation rate of excess carriers, the Arrhenius formula

$$I(T)=I(0)\left(1+CT^{3/2}e^{-E_i/kT}+\sum_k C_k e^{-E_k/kT}\right)^{-1} \tag{3}$$

describes the decrease of the luminescence intensity I with temperature T. E_i is the ionization energy, C the degeneracy factor. In (3) involved are the thermal populations of further excited states (E_k) with degeneracy factors C_k. The equation also implies a constant lifetime of free carriers (Sect. 4.2).

Figure 4 shows the luminescence intensity of the CrB-pairs as a function of temperature. The fit of the data (full lines) with (3) yields the ionization energy of $\sim20\,meV$ – the excited state is located 20 meV from the band edge. For a donor – and CrB is known to act as a donor – the initial state is below the conduction band. Therefore we get for the luminescence ground state a

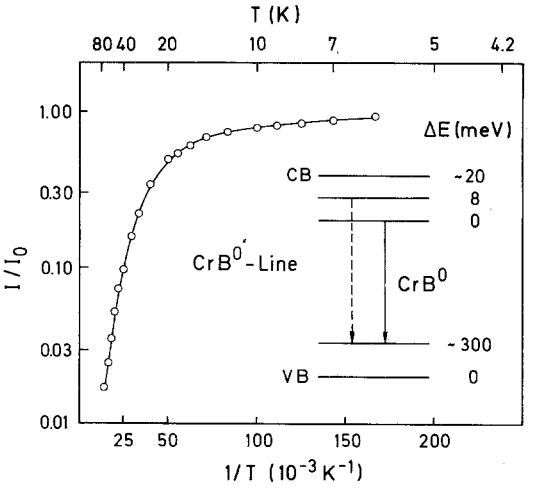

Fig. 4. Temperature dependence of the CrB^0 line. Inserted is the level scheme of the optical transitions

position $E_g - h\nu - 20\,\text{meV} \cong 0.30\,\text{eV}$ above the valence band. The value is in excellent agreement with the CrB-level position at $E_v + 0.28\,\text{eV}$ as determined by various electrical methods [16, 9]. The complete level scheme of the optical transition is inserted in Fig. 4. The fit of the thermal data points to a second excited state 8 meV higher in energy. The corresponding optical transition was observed, but only if uniaxial stress was applied to oriented samples [30] (Sect. 4.2).

3. Optical Spectra Associated with 3*d* Elements

This section gives a survey of the spectra associated with the various 3*d* elements. Based on the concept which was used for the CrB pairs, we will try an identification and characterization of the luminescent defect and compare optical and electrical determined level positions. The problems which arise in center identification are critically remarked. The most important results are summerized in Table 1 and the Figs. 5–8. The table lists the spectral position of the no-phonon line of the lowest excited state, the thermal ionization energy E_i and the luminescence ground state position. The latter value could be compared with the electrical level position of the defect (column 5). The table is completed by the interpretation of the luminescence transitions and some remarks.

According to Figs. 6 and 8, the spectra are classified into two groups. This classification is not only justified by the visual similarity of the spectra but also by common electronic properties, as will be shown in forthcoming sections.

3.1. Investigations on Titanium and Vanadium Doped Silicon

There is only a relatively small number of publications concerning the properties of V or Ti doped silicon (see [5–7, 37] and references therein). It is suggested that both elements have the lowest solubility (around $10^{13}\,\text{cm}^{-3}$ at 1100°C) of the 3*d* elements in Si. Therefore – assuming comparable quantum efficiencies as for the CrB luminescence – only small luminescence signals can be expected.

Independent of used dopants and doping of the starting materials, we could not observe any spectrum which was clearly correlated with titanium. On the other hand, we found a spectrum in Si:V which is shown in Fig. 5. The intensity of the luminescence in our best samples was more than one order of magnitude lower than for CrB, thus comparable detailed studies as for CrB, e.g. measurements in uniaxial stress fields, were not possible. Temperature controlled measurements yielded only a rather weak decrease in intensity up to 100 K. This observation suggests an initial state of the optical transition with a larger ionization energy than for the luminescent single donors CrB, CrGa or Mn_4 (Fig. 6). We cannot give quantitative values for E_i due to the low observable intensity range.

Of the 3*d* elements, V has a rather low diffusivity and therefore only a poor ability to form precipitates or complexes with other impurities in Si during or after sample quenching. Lemke [37, 38] reported that rather high annealing temperatures are necessary for the formation of V complexes. Therefore we tentatively associated the spectrum to interstitial V. V appears in four charge states V^0, V^+, V^{2+}, V^- [8, 37]. The energetic position of the NP line agrees with a transition from an excited state of the singly charged V^+ to its ground state, $V^{2+} \rightarrow (V^+)^* \rightarrow V^+$. The luminescence ground state is located at $E_v + (0.34 - E_i)\,\text{eV}$, the DLTS niveau reported at $E_v + 0.29\,\text{eV}$ [8]. The doubly charged core of V^{2+} could explain the –

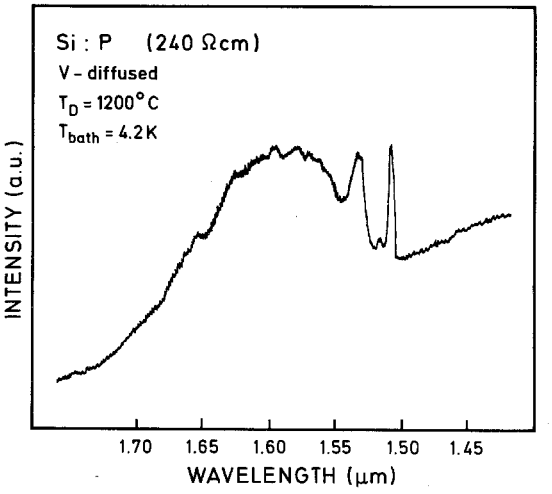

Fig. 5. Spectrum of a vanadium doped sample

compared to CrB, CrGa, and Mn_4 – higher ionization energy E_i.

The difficulties which arise in the investigations of the V luminescence or in finding a Ti spectrum are partially caused by the problems to achieve a reproducible doping of Si with both elements. Extremely low concentrations of oxygen in the diffusion atmosphere reduce or prevent the in-diffusion of both elements but especially of Ti [39, 40]. Therefore further investigations are needed to confirm our results, e.g. on samples where Ti or V will be introduced by ion-implantation and subsequent annealing.

3.2. *Chromium*

The luminescence of the CrB-pairs (Fig. 6 upper part) was already discussed in Sect. 2. We observed another Cr-associated spectrum in Cr-doped Si:Ga (0.7 Ω cm), see middle part of Fig. 6. The luminescence shows striking similarities to the CrB luminescence in many respects. Both spectra are almost equivalent in their absolute intensities (measured with a PbS detector), both no-phonon lines show a rather similar finestructure which points to analogous electronic level schemes [41].

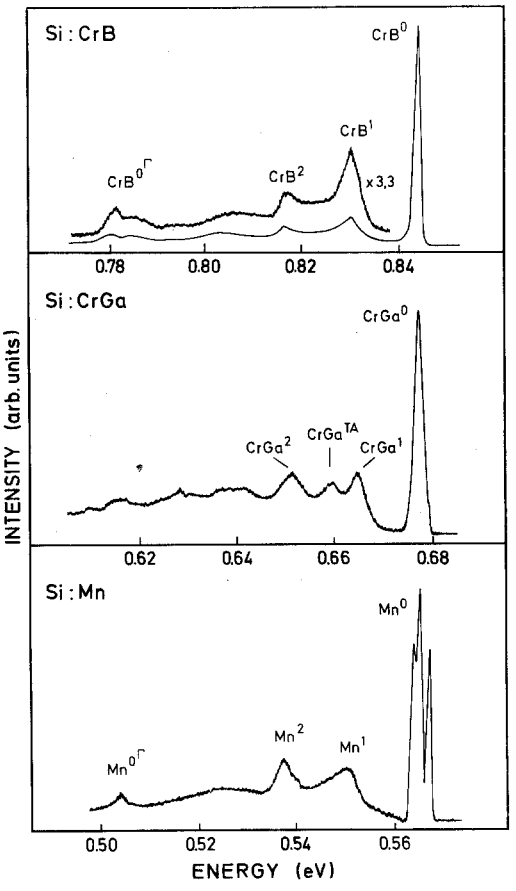

Fig. 6. Deep donor luminescence of CrB (upper), CrGa (middle), and Mn_4 (lower spectrum)

Temperature-controlled measurements yielded an even smaller ionization energy of $E_i \cong 5$ meV (CrB: $\cong 20$ meV), but an almost equivalent prefactor C in (3) was determined. Therefore it is reasonable to associate the spectrum to the CrGa-pairs. If we compare the position of the luminescence ground state – assuming an analogous transition as for the CrB pairs – at $E_v + 0.47$ eV with the electrical niveau at $E_v + 0.46$ eV [9] there is again an excellent agreement of both positions.

The luminescence of CrAl is expected to ly around 2.2 μm since an DLTS level at $E_v + 0.52$ eV is associated to these pairs [9]. Up to now we did not find the corresponding spectrum. Also no luminescence signal of isolated interstitial Cr was found neither in n-type nor in p-type silicon.

3.3. *Manganese*

In Mn-diffused Si also doped with various shallow dopants (B, P) only one clearly Mn-associated spectrum has been observed (Fig. 6 lower part). The luminescence signal fullfills all the criteria given in Sect. 2 to clearly associate it to a Mn center. The NP line Mn^0 appears at an energy of 0.56 eV, roughly half of the band-gap energy. This is the deepest spectrum associated with an extrinsic dopant in Si reported so far. Details of the investigations have been outlined in [31]. Measurements in uniaxial stress fields point to a center with T_d symmetry, either Mn_i or the well known Mn_4 cluster. Based on the characteristic dependence of the luminescence intensity on the doping concentrations of the starting materials, the spectrum was associated to the Mn_4 cluster: The luminescence was only found in p-type Si with low doping concentrations ($< 10^{15}$ cm^{-3}) or moderately doped n-type Si. The detailed dependence of the signal from the phosphorus concentration is shown in Fig. 7. The Mn_4 cluster should be formed mainly from neutral interstitial Mn atoms, since equally charged atoms feel an repulsive Coulomb interaction. At high P concentrations the acceptor level of Mn at $E_c - 0.12$ eV [8, 42] becomes occupied, e.g. Mn_i is negatively charged and the formation of the clusters prohibited. The marked Mn_4 stability sectors in Fig. 7 are calculated using the acceptor level of Mn_i or two arbitrary level positions at $E_c - 0.2$ eV or $E_c - 0.05$ eV and assuming a chemical reaction of fourth order (left boundary) – as it is expected for the reaction $4\,Mn_i \rightarrow Mn_4$ – or second order (right boundary) – still allowing the participation of some charged Mn atoms in the reaction. The data agree well with the assumption that Mn_4 is formed purely of neutral interstitial Mn.

Annealing experiments showed that the center could be stable up to temperatures of more than 200° C

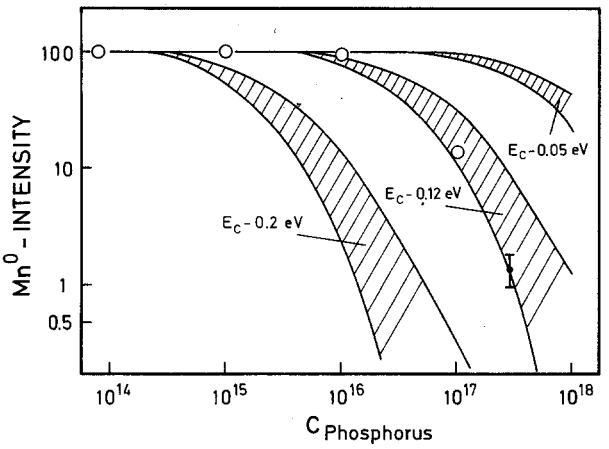

Fig. 7. Mn^0 intensity as a function of phosphorus concentration (indicated by circles). The marked regions are stability regions for Mn_4 clusters, calculated with the Mn acceptor level ($E_c-0.12$ eV) and two arbitrary level positions

[31], but also that the annealing behaviour depends strongly on the special sample preparation technique and sample history. Nevertheless, the high thermal stability of the luminescent center also points to the Mn_4 cluster, since interstitial Mn is rather unstable even at room temperature and likes to form clusters or even larger precipitates at elevated temperatures [8, 42, 43]. In addition, the Mn_4 clusters were observed in the samples with EPR [44].

The ionization energy of the center in the excited state (Table 1) derived from thermal data is 30 meV which is almost equivalent to the effective mass value of donors in silicon (31.3 meV) [45]. The luminescence ground state is then near midgap – assuming a donor transition at $E_v+0.59$ eV. The level positions reported for the Mn_4 donor in literature are quite controversily [36, 42, 43, 46–50]. Hall – combined with EPR – investigations of Feichtinger et al. [36, 42] yielded a level at $E_c-0.28$ eV, on the other hand photo EPR results [46] and combined EPR and DLTS data (level at $E_c-0.54$ eV) [43] as well as the Hall measurements of Carlson [47, 48] point to a midgap level position. The luminescence data may be taken as a further evidence that the Mn_4-donor level is located around midgap.

3.4. Iron-Associated Spectra

The first luminescence investigations on 3*d* elements in Si were reported from Weber and Wagner in 1980 and dealt with the luminescence of iron complexes [25]. These authors observed various new line-systems in n- and p-type silicon which seemed to be iron correlated. Whereas for spectra in n-type silicon no or only tentative center identifications were proposed, there was strong evidence that a spectrum in boron doped starting material was due to the FeB pairs. Rather analogous spectra even with similar annealing behaviours were observed in In- and Tl-doped Si after thermal quenching of samples [26, 29, 51–53]. Therefore it was proposed by Sauer and Weber [29] that all these luminescent centers belong to the class of iron acceptor pairs. Two of the spectra – those in Si:B and

Table 1. Optical transitions of 3*d*-TM centers in Si. The spectra are represented by their NP line. E_i is the thermal ionization energy obtained from intensity decrease with T

TM complex	NP $h\nu$ [eV]	E_i [meV]	Level position from		Remarks
			Lumi	DLTS/Hall [eV]	
Ti	–	–			No luminescence was observed
V_i?	0.822	>30?	≃0.3	$E_v+0.29$	$V_i^{2+}\rightarrow V_i^+$
Cr_i:					
CrB	0.844	~20	0.30	$E_v+0.28$	$CrB^+\rightarrow CrB^0$
CrGa	0.677	~ 5	0.48	$E_v+0.47$	$CrGa^+\rightarrow CrGa^0$
Mn_i:					
Mn_4	0.56	~30	0.59	$E_c-0.55$	$Mn_4^+\rightarrow Mn_4^0$
Fe_i:					
Fe?	0.734	–			Centers not yet identified
"FeB"	1.067	15			
"FeTl"	1.087	27			
Co	–	–			Form precipitates, no luminescence
Ni	–	–			
Cu	1.015	32	0.12	$E_v+0.10$	Modell: Cu–Cu pair

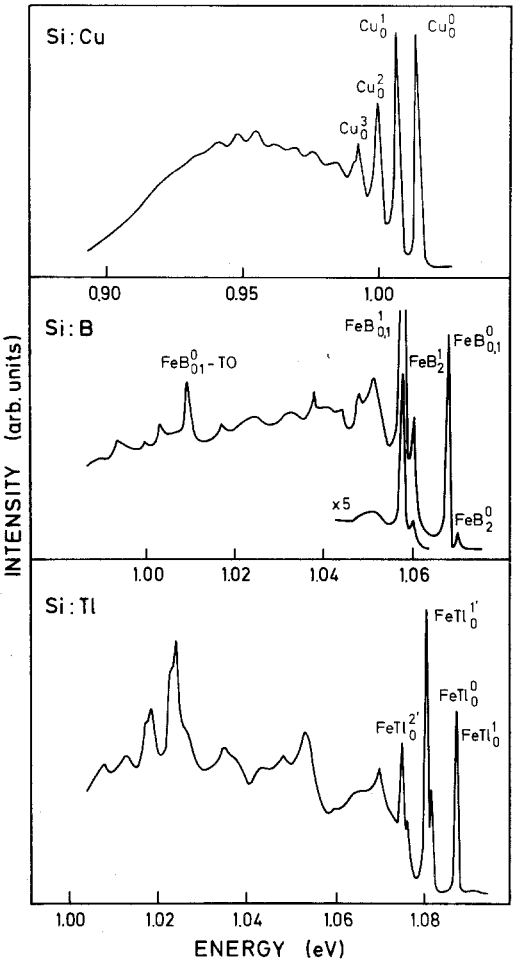

Fig. 8. Spectra of isoelectronic centers associated with Cu and Fe. The Fe lines are named due to a previous suggestion with Fe-acceptor pairs in B and Tl doped Si

Si:Tl – are shown in Fig. 8. The lines are marked with FeB or FeTl (according to [29]) reflecting this interpretation. The Fe associated lines in Si:In and Si:Tl are of special interest, since the luminescent centers exist in two different configurations which can transform into each other. Especially for the Tl center the luminescence studies yielded a detailed model for the mechanism of reorientation [54–56]. Its trigonal symmetry at low temperatures, i.e. most probably the ⟨111⟩-orientation of a pair, is changed to rhombic, i.e. an ⟨100⟩-alignment of a pair defect, between 15 and 20 K. A similar reorientation was observed for FeAl-pairs in Si by DLTS [57]. For more details concerning these most unusual defects we refer to [54–57]. (Note: The labeling of the lines is different in these references, the luminescence systems are named Si:InQ and Si:TlQ.)

Recently, the Fe correlation of the spectra was put in question. On one hand Schlesinger and McGill [58] found a dependence of the FeIn and FeTl luminescence signals on iron doping, but on the other Watkins and coworkers [55] have not found any influence of iron doping on the intensity of the spectra. A strong argument against interstitial iron being a constituent of the defects is the lack of iron related isotope shifts in the phonon replicas of the FeB [59] or the FeIn spectrum and a Fe spectrum in n-type Si [60]. After doping with iron 54 or 56 isotopes, respectively, neither a shift of the NP lines nor of the phonon replicas was observed, although at least for the intense replicas a well resolvable line shift could be expected.

The maximum concentration of the luminescent "FeB"-center was estimated in [61] to be 10^{12} to $10^{13}\,cm^{-3}$, well below the concentration of the electrically active FeB-pair. Mohring et al. [61] therefore stated that Fe and B are needed for center formation but that the center is not identical to FeB.

Our recent results obtained on samples with background dopings of boron and phosphorus in the range of 10^{13} to $10^{18}\,cm^{-3}$ and Fe doped with the different diffusion techniques described in Sect. 1, were also quite controversal. However, iron indeed seems to be necessary for formation of luminescent centers in n-type Si or for "FeB". The absolute intensities of the spectra in identically prepared samples showed a scatter of more than two orders of magnitude. DLTS or EPR measurements on interstitial iron or FeB-pairs give quite reproducable results with concentrations at 1100°C of $5 \times 10^{15}\,cm^{-3}$ [4, 10]. Therefore the spectra cannot be associated to these well defined iron centers. For the FeB luminescence this is also supported by the fact that the luminescence signal disappears rapidly in Si with B concentrations above $10^{16}\,cm^{-3}$, although – according to the law of mass action – the pair should be stable at these high B concentrations. The luminescence of CrB is observable at an even higher boron content [41]. On the other hand, the observation may indicate that the center contains iron. If all Fe atoms are bound in FeB-pairs no ones are left to form the luminescent center. The luminescence decreases since the B concentration exceeds that of Fe in the samples.

Up to now there is no model for the chemical structure of the centers. It may be that intrinsic defects participate at the defects or that iron is involved on the substitutional lattice site. The latter possibility could explain the lack of large isotopic shifts in the phonon replicas, since it is assumed that mainly the interstitial TM is responsible for the local mode replicas (Sect. 5).

3.5. Cobalt, Nickel, and Copper

The three metals Co, Ni, Cu are the most rapidly diffusing of the 3*d* elements in Si. This high diffusivity – their diffusion coefficients at 1100°C are about $10^{-4}\,cm^{-2}/s$ – and their low solubility at room temperature – around one atom cm^{-3} compared to

$10^{17}\,cm^{-3}$ at 1100°C – is responsible for their tendency to form precipitates during quenching. Almost no atoms could be kept isolated on interstitial lattice sites at room temperature [4, 5, 62–64]. This explains the controversy in the positions of the electrical levels reported in [5–8, 65] – there are no levels which are undoubtly correlated with the isolated interstitial metals. A quite reproducable level was reported for Cu in low concentrations ($5\times10^{13}\,cm^{-3}$), which however may belong to a Cu complex [8]. EPR investigations yield the same negative results, only a Ni complex associated signal was observed [4].

The luminescence studies of the elements are well beyond these results. Our search for Ni- and Co-related spectra was not successful. Bergholz [66] reported the observation of CoB-pair formation with Mössbauer spectroscopy in highly B doped Si-starting material. We especially looked for luminescence of the pairs, but did not observe a CoB correlated spectrum – in agreement with the fact that no DLTS signal of CoB was found [65].

Contrarily to the situation in Co- and Ni-doped Si, diffusion of Cu in Si yields the upper spectrum in Fig. 8. The luminescence was first observed by Minaev et al. [67], but the identification with a Cu center was first achieved by Weber et al. [27] and independently proposed by Watkins and coworkers [28]. The spectrum is up to now the only one of the 3*d* metals where isotope shifts in the no-phonon line and phonon replicas could be observed and thus the participation of Cu in the luminescent center is directly proved [27]. Due to the trigonal center symmetry determined from stress measurements and the kinetics of center formation – the luminescence intensity depends quadratic on the Cu concentration – Weber et al. [27] associated the spectrum to a Cu–Cu pair, possibly Cu_s–Cu_i. The position of the luminescence ground state (Table 1) is in agreement with the above mentioned Cu-associated DLTS level. Thus luminescence and DLTS possibly observe the same center.

4. Electronic Properties of the Luminescent Centers

4.1. Iron- and Copper-Related Spectra: Isoelectronic Excitons

In Figs. 6 and 8 the 3*d*-TM spectra have been already divided into two groups. We will now justify this classification and work out common and distinguishing features of the optical transitions. Let us first deal with the spectra of Fig. 8, the Cu–Cu, "FeB", "FeTl" plus the "FeIn" luminescence. All these spectra show the specific fingerprints of radiative recombination of isoelectronic excitons, as they are well known from luminescence systems in III/V-semiconductors [68, 69], e.g. GaP:N. Recently, several spectra due to isoelectronic excitons were also observed in Si, the first one being the ABC exciton [71]. An isoelectronic exciton consists of an electron-hole pair which is bound to an isoelectronic center by a short range potential. Group IV impurities are isoelectronic to Si, but there may be also impurity complexes, which show isoelectronic properties.

Table 2. Lifetimes τ and localization energies E_{BX} of isoelectronic and acceptor-bound excitons

Exciton at	E_{BX} [meV]	τ [μs]	Ref.
FeB	88	30	[41]
FeIn	37	200	[52]
FeTl	68	52	[52, 54]
CuCu	140	600	[28]
B	4.2	1.055	[75, 73]
In	14	2.7×10^{-3}	[75, 73]
Tl	44	2.8×10^{-4}	[75, 76]

Well-studied examples for such complex-centers are Li–O–Li in GaP [72] or a Li_4 cluster in irradiated Si [35]. These centers introduce no net charge into the crystal and their ground state – then no exciton is bound at the defect – is therefore a spinless state. A first indication that the optical transitions are due to isoelectronic exciton decay comes from decay times of the spectra which are unusually long for Si (Table 2). The lifetimes of excitons bound to donors or acceptors in Si is limited by the nonradiative Auger process, e.g. for donors the electron takes over the recombination energy and the momentum of the e–h pair and is highly excited into the conduction band [73, 74]. The isoelectronic exciton is only a two particle system. Therefore such an Auger process is not possible, the lifetime is usually determined by the radiative recombination probability of the exciton. In Table 2 the decay times of the three luminescence spectra of Fig. 8 and "FeIn" are listed together with the time constants of the B, In, and Tl exciton decay and the localization energy, $E_{BX}=E_g-E_X-h\nu=1.1552\,eV-h\nu$, of all bound excitons BX (E_X: FE binding energy). Since the BX Auger time constant is a function of the acceptor ionization energy ($\tau\sim E_i^{-4.6}$) [73] and with Haynes' rule [20], $E_{BX}\sim0.1\,E_i$, also a function of E_{BX}, the Tl–BX has the shortest lifetime. The 3*d* excitons have an even larger localization energy, but they have lifetimes of 30 up to 600 μs. Therefore we can exclude the possibility of effective nonradiative Auger recombination for these centers – as it is expected for isoelectronic excitons. The optical transitions should have a high quantum efficiency and indeed the luminescence signals are rather intense although the center concentrations are estimated to be very low ($<10^{13}\,cm^{-3}$) [61].

The level scheme of the isoelectronic exciton is constructed by coupling the angular momenta of the conduction band electron ($S=1/2$) and the valence band hole ($S=3/2$). For spherical symmetry one gets two states with total angular momenta $J=1$ and $J=2$. The actual symmetry of defects in silicon is not spherical but T_d or even lower for extended defects. The crystal field or internal fields of lower symmetry lifts the degeneracies of the $J=2$ and $J=1$ exciton states. The states are then characterized by the representations of the respective point group [77]. However, the crystal field splitting is often very small. Then the spherical or axial approximation describes the level scheme in an adequate manner. Transitions occur from the different exciton states to the $S=0$ ground state of the defect. The $J=2\rightarrow 0$ transition normally shows low intensity, since it is dipole forbidden.

The level schemes of the three centers of Fig. 8 derived from Zeeman and stress measurements are well explainable in the model of isoelectronic excitons in the spherical approximation. We observe transitions from exciton states with $J=1$ and $J=2$ either still degenerated or split by the internal strain field of an axial defect (the levels are then characterized by the magnetic quantum number m_J) to the defects ground state with $J=0$.

Mohring et al. [61] associated the FeB_1^0 line to the $J=1\rightarrow 0$ transition whereas the FeB_0^0 line corresponds to the dipole forbidden transition from the $J=2$ state. In Fig. 8 both lines fall together. The situation for the Cu–Cu pair is rather similar. Only the angular dependence of polarizations of Zeeman lines or measurements in uniaxial stress fields showed that the centers symmetry is trigonal [27, 29].

Contrary to these two centers the level scheme of "FeTl" is strongly affected by the trigonal center axis. The $J=2$ or $J=1$ exciton states are split into sublevels separated by several millivolts and characterized by the magnetic quantum numbers m_J [54, 56]. The trigonal symmetry of the center is clearly seen in the angular dependence of the Zeeman splitting of the $TlFe_0^0$ line (Fig. 9). The solid lines are calculated for the $m_J=\pm 2\rightarrow 0$ transition at a trigonal center with a $g_{\parallel}=2.3$ value parallel to the defect axis, whereas $g_{\perp}=0$. This means that a field aligned parallel the defect axis causes a twofold splitting of the $FeTl_0^0$ line since it lifts the degeneracy of the $m_J=\pm 2$ state, whereas a field perpendicular the axis has no effect on the electronic state. The four different center types – according to the four ⟨111⟩ crystal directions – are distinguished by the projection of the magnetic field on their axis. Only for H parallel ⟨100⟩ all centers are equivalent – the splitting in Fig. 9 is then simple and twofold. For a more detailed discussion of the "FeTl" or "FeIn" level schemes we refer to [54, 56].

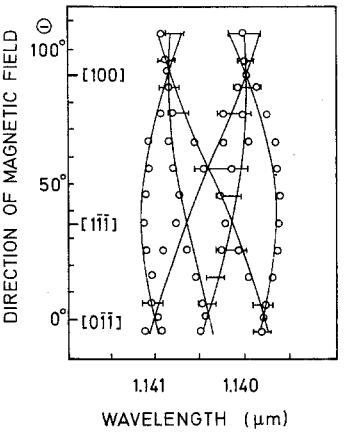

Fig. 9. Angular dependence of the Zeeman splitting of the FeTl line

The thermal ionization energy E_i (Table 1) of th excitons is around 30 meV, e.g. similar to the ionizatio energy of the effective mass donor or acceptor in S The localization energy of the excitons, on the othe hand, is much larger (Table 2). Therefore one particle according to the model of Hopfield, Thomas, an Lynch [70] – either the electron or the hole is deepl localized at the center, the second bound by Coulom attraction. Hopfield and co-authors [70] distinguis between pseudo-donors – the hole is deeply bound and pseudo-acceptors in the inverse case. The detaile analysis of the luminescence data indicates that a centers are pseudo-donors [27, 52, 61, 54].

4.2. CrB, CrGa, *and* Mn_4
Capture Luminescence of Deep Donors

We will now discuss the level schemes of the spectr shown in Fig. 6. Again – as for the isoelectronic center – the obvious similarity of the three spectra is strikin and again there seems to be a complete analogy of th optical transitions.

Let us first consider some differences to the spectr of the isoelectronic centers of Fig. 8. The phono coupling is much lower here (Figs. 8 and 6) – the nc phonon line is the dominant transition. The absolut intensity of the spectra is two to three orders c magnitude lower than for the isoelectronic 3*d* center although the center concentrations (aroun $10^{15}\,cm^{-3}$) are more than a factor of ten highe Therefore the quantum efficiency of the transitions a these centers should be rather low contrary to th expectation for classical isoelectronic exciton (Sect. 4.3). The NP line of each of the spectra shows complicated finestructure, e.g. this is shown for th Mn_4 line in Fig. 10. The relative intensities of thre (1, 3, 4) of the four NP transitions are clearly indepen dent of the measurement temperature, so the corre sponding states are not occupied according to

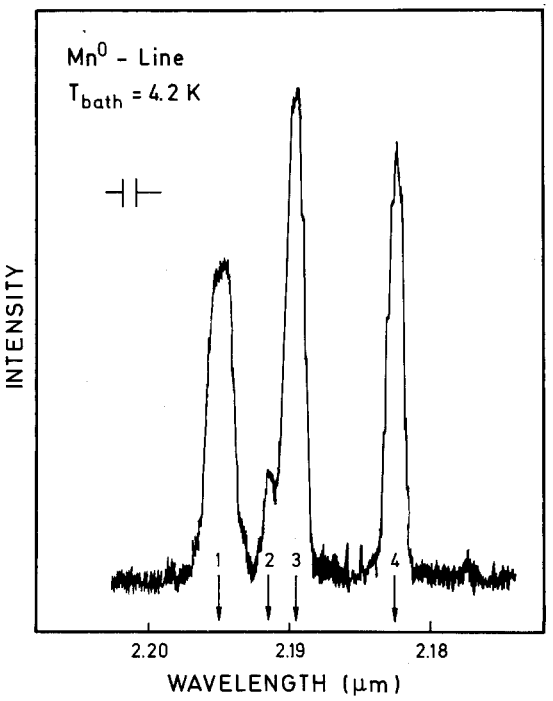

Fig. 10. The fine structure of the Mn^0 line

thermal distribution [31]. This suggests that it is the final state of the transitions which is split into several sublevels in contrast to the $S=0$ final state of an isoelectronic center.

Within the discussion of the CrB luminescence (Sect. 2.3) it was assumed that the spectrum is due to an optical transition from a rather shallow excited state of a donor to its deep ground state. However, theoretical calculations (method of finite cluster calculations) of 3*d*-metal level schemes predict a ladder of deep states within the forbidden band gap [78, 79]. The luminescence spectra could then also correspond to internal transitions between such states. The initial state is then not necessary shallow and the ionization energy E_i of Table 1 becomes questionable, since there are other mechanisms which could cause a similar temperature dependence of the NP lines of the spectra. We will now discuss these mechanisms and confirm our previous interpretation:

1) The coupling of the optical transitions to local modes or lattice phonons may reduce the NP intensity with increasing temperature, since the intensity of the NP line is "transferred" to the phonon side bands.

The effect was in detail studied by Sauer and Weber [80] for the Cu–Cu pair. The authors have found that the NP intensity is little affected. For CrB, CrGa, and Mn_4 the phonon coupling strength is smaller than for Cu–Cu (Sect. 5), therefore the effect is even smaller – we estimated a negligible change in intensity of 2% between 10 and 60 K [41].

2) Additional nonradiative recombination channels may be switched on with increasing temperature.

It is well known that many transition metal impurities act as very efficient recombination centers. If such recombination channels are thermally activated (e.g., the multiphonon process) most of the optically generated free carriers may recombine via these radiationless paths and not via the optical transitions. Since the generation rate of free carriers (the excitation laser power) is constant, this must reduce the luminescence intensity. The mechanism also must result in a reduction of free carrier lifetime. Hangleiter [12, 13] has measured excess carrier lifetimes in Si doped with 3*d* elements, e.g. the luminescent CrB pairs. He found that the lifetime is specific on the dopant and its concentration but is nearly independent of temperature in the range from 20 to 60 K, where the strong intensity decrease of our spectra occurs. This excludes Mechanism 2. being responsible for the intensity decrease.

3) The internal quantum efficiency of the optical transitions may be reduced by thermally activated multiphonon transitions within the system of center states.

The temperature dependent branching of the recombination in a radiative and nonradiative path at the luminescent center can be only roughly estimated assuming a multiphonon transition [41, 81]. For the rather low Huang Rhys factor of $S<1$ and the phonon energy of about 13 meV of all spectra, however, it seems to be very unlikely that there could be a strong effect. Only if there would be further states with large lattice relaxation effects ($S \gg 1$) one would expect a decrease in intensity of the observed orders of magnitude [41]. Up to now there is no experimental evidence that such states exist. Therefore the most straightforward explanation for the temperature dependence of the spectra is still the ionization of the centers in their excited states.

There are other indications which support the interpretation. The investigation of the CrB^0 and Mn^0 line in uniaxial stress fields yielded similar splittings as those of shallow donor e or t_2 states. For the CrB^0 line (Fig. 11), the splitting indicated by solid lines is due to the orientational degeneracy of the trigonal CrB pair [30]. The center of gravity of these lines in each stress direction ($\langle 100\rangle$: 5.1 meV/kbar) nearly follows the shift of the conduction band edge under stress ($\langle 100\rangle$: 5.8 meV/kbar [82]). This similarity suggests that the excited state of the CrB^0 line is coupled to the conduction band. Additional splittings marked by dashed lines correspond either to electronic splittings or an high energy excited level of the CrB^0 line. This level 8 meV above the CrB^0-initial state was already shown in Fig. 4.

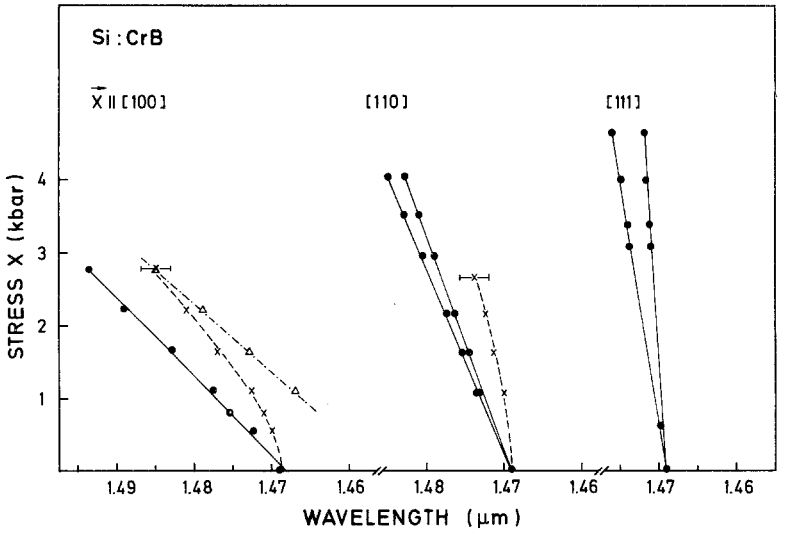

Fig. 11. Stress splitting pattern of the CrB^0 line

If we add to our arguments the fact that there is a complete agreement between the luminescence ground-state and the electrical-level position for the three centers, the previous interpretation is confirmed and we may conclude:

The observed spectra of CrB, CrGa, and Mn_4 are due to optical transitions from rather shallow effective mass like states in the deep ground state or at least states nearby the ground state of the defect.

The fine structures of the no-phonon lines reflect the electronic occupation of the 3*d* shell of the transition metals. Following the model of Ludwig and Woodbury [14] for an interstitial TM all 4*s* electrons are transferred to the 3*d* shell. A small crystalfield splits the degenerated *d* states into a twofold *e* level and a threefold t_2 level, with the t_2 state being lower in energy. The levels are occupied according to Hund's rule, resulting for the ground state in a high spin state. Recent theoretical calculations predict low spin states for some of the early and late TM [83, 84] in disagreement with the model of Ludwig and Woodbury [14], but for the elements considered here the high spin states seem to be confirmed. In the excited state an electron ($S=1/2$) is bound in the Coulomb field of the positively charged center. The electronic configuration is given by coupling $S=1/2$ of the electron to the momenta of the positive core states (constructed with the model of Ludwig and Woodbury). This is similar to a model proposed by White [85] to explain the NP fine structure of Cr luminescence in GaAs. White applied an excitonic picture: The hole of the exciton is bound deeply in the *d* shell of the center, the electron in the Coulomb field of the localized hole.

For interstitial Mn the configuration is ($5t_2$, $2e$). However, for Mn_i in the Mn_4 cluster one electron is transferred from e to the t_2 level ($6t_2$, $1e$) [42]. This yields a total spin $S=1/2$. The ground state of Mn_4 is formed by coupling $S=1/2$ of the four Mn_i atoms to $S=0$, 1, 2 states, the $S=2$ state being lowest in energy (known from EPR) [42]. The three ground states may cause the three non thermalizing fine-structure lines in Fig. 10 [31]. A splitting in the excited states which is responsible for the additional line and the line broadenings is expected according to Whites model, but the electronic configuration of Mn_4^+ is not known. Zeeman measurements could be helpful to identify the quantum numbers and to derive a complete level scheme for the optical transitions, but are difficult to do, since the intensity of the spectrum is rather low.

Very similar is the situation for CrB or CrGa. Cr^+ ($2e$, $3t_2$) (the ground state configuration of the Cr^+B^- pair) has a total spin $S=5/2$ which is quantized (m_j) along the pair axis. The energy differences of the sublevels are given by $\Delta E=Dm_j^2$. For CrB $D=0.01$ meV [14] is too small to give well resolvable splittings of the CrB^0 line. The CrB^0 fine structure therefore is mainly due to splittings in the excited state. In [30] it was assumed that the transition occurs at the B atom ($B^0 \rightarrow B^-$) but calculations of Vogl [86, 87] have shown that the level Cr^+/Cr^{2+} which lies within the valence band for Cr_i is pushed into the band gap for the pairs. The excited state is then constructed by coupling the $S=1/2$ electron to Cr^{2+} ($1e$, $3t_2$, $S=2$). To explain the splittings *D* should be around 0.2 meV. For CrGa the considerations are analogous and only the magnitude of *D* is changed as well in the ground as in the excited state. The fine structure of the CrB and CrGa–NP line are therefore very similar [41].

4.3. Recombination Centers

Many of the 3*d* centers in Si act as very efficient recombination centers. Hangleiter [12, 13] has shown

with time-resolved photoluminescence measurements (near band-gap luminescence of free excitons or free carriers) that this holds also for very deep sample temperatures, e.g. 20 K. The lifetime of the optically generated carriers in Si:B (1 Ω cm) doped with Cr ($1 \times 10^{15}\,cm^{-3}$) at these temperatures is around 1 ns [88]. For Mn-doped Si no time-resolved measurements were reported to date, but the luminescence analysis gives evidence that the Mn_4 cluster is an effective recombination center.

Samples which show a strong signal of Mn_4, have no or only very weak near band gap luminescence of free excitons (FE). Since the FE intensity is a measure for free carrier concentration, an effective recombination channel had been introduced with Mn doping, which reduces the FE concentration under stationary conditions. After sample annealing at temperatures above 200°C the Mn_4 luminescence decreases and simultaneously the FE signal reappears.

In isothermal annealing experiments the Mn_4 intensity shows an exponential decay with a time constant $\tau = 11.7$ min at 265°C [41]. If one assumes that the concentration of Mn_4 atoms is proportional to the Mn_4 intensity he can calculate the FE intensity I as a function of annealing time using the rate equation for stationary conditions:

$$\frac{dn_x}{dt} = 0 = g - \frac{n_x}{\tau} - Cn_x\{Mn_4\} \tag{4}$$

with g a constant exciton generation rate, τ an effective FE lifetime which contains all recombination channels but Mn_4, n_x the FE concentration and C the capture coefficient of FE for Mn_4:

$$I(t) = I(\infty)\,(1 + Be^{-t_A/11.7\,\mathrm{min}})^{-1}. \tag{5}$$

The result of experiment and calculation (solid line) is depicted in Fig. 12. Important is the fact that the increase of FE intensity and the decrease of the Mn_4 signal shows the same time constant and that the high annealing temperatures necessary for the Mn_4 anneal out are very characteristic. Most of the pair centers (e.g., CrB or FeB) dissociate well below 200°C. Therefore we may conclude that it is indeed the luminescent Mn center which acts as an effective recombination center.

The Mn_4 clusters, CrB and most probably CrGa are recombination centers, contrarily to the isoelectronic centers of Fig. 8, which bind excitons with very long lifetimes (Table 2). These long lifetimes and the low center concentration result in a rapid saturation of the luminescence intensity with excitation power (Fig. 13). The high intensity of the optical transitions must be caused by a high quantum efficiency of transitions at these centers, excluding effective nonradiative recombination paths.

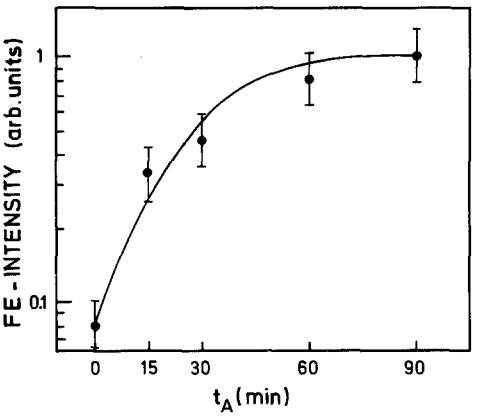

Fig. 12. Increasing of the free exciton (FE) intensity with annealing time (T_A=265°C) in Mn doped Si (B=11.5)

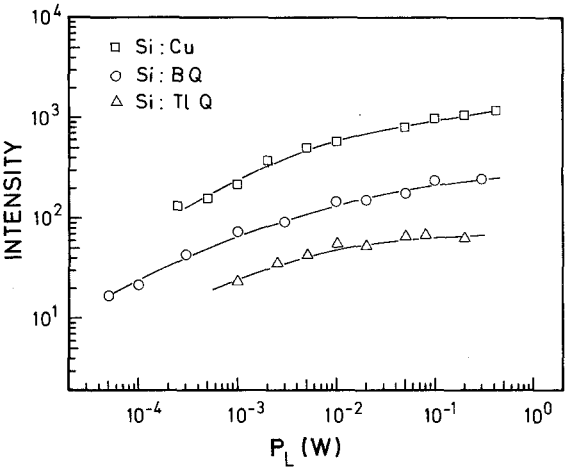

Fig. 13. Cu_0^0, FeB_0^0, and $FeTl_0^0$ intensity as a function of laser power. The spectra are shown in Fig. 8

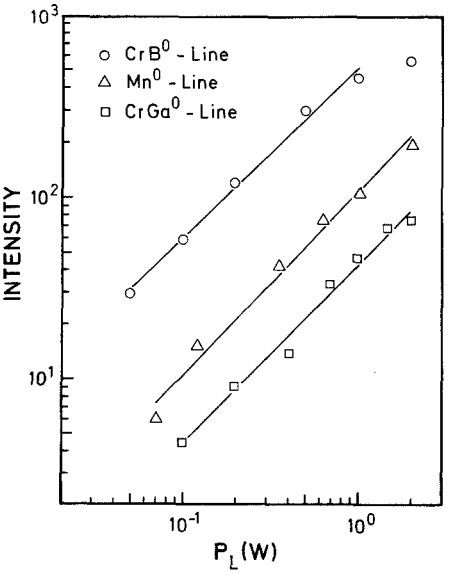

Fig. 14. Intensity of the CrB^0, $CrGa^0$, and Mn^0 line versus laser power

The luminescence intensity of CrB, CrGa or Mn_4 is more than two orders of magnitude lower than that of the isoelectronic excitons, although the center concentrations are even higher. Since these centers are effective recombination centers the optical transition cannot be the main path for recombination. Nonradiative transitions may dominate at these centers. The difference between the two groups is also seen in the saturation of the luminescence with laser power (Figs. 13 and 14). Contrary to the isoelectronic excitons no saturation is observed here, the intensity is strictly linear due to the effective recombination channels and the higher center concentrations.

5. Phonon Structure of the Spectra

All the spectra discussed in the previous sections show phonon side bands which are due to the excitation of lattice phonons and localized vibrations during the optical transitions. The energies of the electronic defect states are affected by the atomic position and vice versa the atomic positions are a function of the distribution of electrons, which is different for different electronic states. Excitation or recombination between defect states therefore causes re-arrangements of atoms in the defects surrounding. This results in lattice vibrations if in an extended region phonons are excited or vibrations localized in the near surrounding of the defect, e.g. for an interstitial TM the TM itself may vibrate. The intensity distribution of the phonon sideband due to lattice phonons is determined mainly by the density of lattice phonon states [89]. There are maxima around 60 meV (TO or O^{Γ}), 20 meV (TA) or 40 mV (LA). Broad structures in the spectra correspond to these energies.

The localized vibrations are often sufficiently described in a configurational coordinate diagram for one (or several) vibrational mode with typical energy $\hbar\omega$ (Fig. 15) [90, 81]. The potentials in the ground (V_G) and excited state (V_A) are shifted by Q_0 in their equilibrium positions. The eigenvalues of the harmonic oscillator

$$E_n=(n+1/2)\hbar\omega \tag{6}$$

form a ladder of vibronic states with the energy separation $\hbar\omega$. The new equilibrium position in the excited state causes an energy relaxation

$$E_R=m\omega^2Q_0^2=S\hbar\omega, \tag{7}$$

which is also expressed in multiples of $\hbar\omega$ by the Huang Rhys factor S. For large S – strong phonon coupling – the energies of the electronic states are strongly affected by lattice relaxation. In luminescence one observes at low temperatures ($kT \ll \hbar\omega$) transitions from the lowest excited state ($m=0$) in the different ground states n.

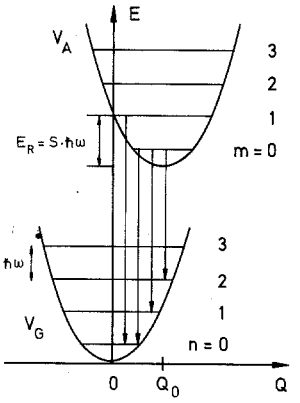

Fig. 15. Configurational coordinate diagram for optical transitions from vibrational levels of an excited electronic state in those of the ground state. For details see text

This explains the equidistant linesystems in Figs. 6 and 8. (More distinct in Fig. 8.)

The relative intensity I_{0n} of the n^{th} local mode and the no-phonon line I_{00} are determined by the phonon coupling strength and is given by [90, 81].

$$I_{0n}/I_{00}=S^n/n! \tag{8}$$

or

$$\sum_n I_{0n}/I_{00}=e^S. \tag{9}$$

Up to now only one normal mode was recognized, but there may be several vibrations with different symmetries. For each mode i we can define a S_i with the total $S=\sum S_i$. For a continuum of modes – such as a band due to lattice phonons – Eq. (9) can be used to define S, but the summation has to be substituted by an integration.

It is obvious from Figs. 6 and 8 that the two classes of spectra show very different coupling strengths S. The total S of the isoelectronic spectra is in the region of 2 to 3, whereas only 0.6 for the Mn and Cr luminescence bands. Vanadium shows with $S\sim 4$ the highest phonon coupling strength of the mentioned spectra. For the spectra of Cu and FeB only one defect vibration is seen in Fig. 8, whereas for FeTl clearly two different local modes with 5.3 and 6.5 meV can be distinguished. For the Cu spectrum also different local modes were reported [28], however, these are not resolved in Fig. 8.

The rather small S values of all spectra indicate low lattice relaxation effects between ground and excited states. The level positions are only slightly changed by lattice relaxation. The energy E_R is – even for V with $S=4$ – only in the order of 60 meV, for the deep donor transitions of Fig. 6 below 30 meV. Therefore the electronic level schemes of the centers seem to be only little affected by lattice relaxation.

Table 3. Vibrational energies $\hbar\omega$ of luminescent defects and the scaled energy $\hbar\omega^*$. The mass m_i and diffusion barrier H_m for each interstitial element is also included

Complex	$\hbar\omega_i$ [meV]	Ref.	$\hbar\omega_i^*$ [meV]	m_i	Hm_i	Ref.
V_i	~14	[41]	13.7	51	>1	[5]
CrB	13.6	[30]	13.6	52	1	[4]
CrGa	13.0	[41]	13.6	52	1	[4]
Mn_4	14.5	[31]	13/11	55	1/0.63	[94, 93]
CuCu	7	[27, 29]	8	64	0.43	[4]
Li_4	32.2	[95]	30.1	7	0.66	[4]
Au?	~ 3	[96]	4.4	197	0.4	[99]

Phonon Energies

Sauer and Weber [29] proposed that in the TM complexes it is solely the interstitial metal which is responsible for the local mode replicas. They argued in analogy to the modes of Li-acceptor pairs which were observed by ir absorption [92]. The phonon energies of these pairs show well resolvable isotope shifts due to Li isotopes, but no ones due to different acceptor isotopes. The phonon energies of the identified $3d$ centers derived from luminescence ly all in the small energy region from 14.5 to 13 meV although the TM are involved in very different complexes. Only for the CuCu pair the value is 7 meV which is considerably lower (Table 3).

In the very simple model that the interstitial transition metal of mass m_i moves in a harmonic potential and that for all centers similar vibrational modes are excited the phonon energies can be compared if the strength of the potential is known.

The diffusion barrier H_m might be a measure for the coupling strength of the TM atom to the surrounding Si atoms. This is demonstrated in Fig. 16. To diffuse from one to the next T_d interstitial site at distance a_0 the TM has to jump over the barrier of height H_m. In the harmonic approximation the barrier height and the force constant D are correlated by

$$H_m = Da_0^2/8 . \tag{10}$$

Clearly the harmonic potential reflects not the real potential shape especially around $a_0/2$ but the proportionality of H_m and D is expected to hold also for more realistic situations, e.g. for atoms with such similar properties as the $3d$ metals [91].

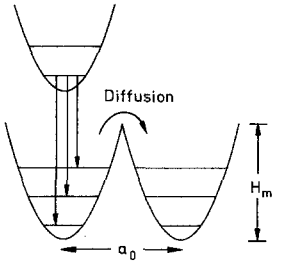

Fig. 16. Diagram which shows the connection of diffusion barrier and phonon energy

With (10) we can estimate the phonon energies of the different $3d$ complexes using the vibrational energy of the CrB pair as a standard

$$\omega_i^* = \omega_{CrB}(H_{mi}/H_{mCr} \times m_{Cr}/m_i)^{1/2} . \tag{11}$$

In Table 3 we have listed beyond $\hbar\omega$ the masses of the $3d$ elements m_i, the diffusion barrier H_m and the scaled phonon energy $\hbar\omega_i^*$. The agreement of $\hbar\omega_i^*$ and $\hbar\omega_i$ is surprisingly good so that the simple model seems to describe the real situation in an adequate manner. Especially the lower phonon energy of the Cu complex is explained with the low diffusion barrier which points to a weak potential.

We have so far neglected the partners of the $3d$ elements in the complexes. Indeed there is an influence on the vibrational energy as could be seen for CrB and CrGa. For Mn_4 new diffusion data [93] point to a lower diffusion barrier of 0.63 eV which reduces the $\hbar\omega^*$ value to 11 meV still in acceptable agreement with $\hbar\omega$. Indeed the Mn_4 complex seems to be the most stable of the luminescent complexes and the electronic configuration of Mn_i in the cluster is changed (Sect. 4.2). Therefore the local mode energy may be somewhat increased.

We have tried to apply our considerations to other luminescent centers in Si which may contain elements on interstitial sites. A prominent example is a Li center ascribed to a Li_4 cluster [35]. The phonon replicas with lowest vibrational energy appear 32.2 meV (Li^7) or 34.2 meV (Li^6) below the NP line and show well resolvable isotope shifts due to Li [95]. A spectrum associated with Au in Si is reported but the structure of the defect is not known [96, 97]. The center could not be identified with the electrical active Au ascribed to substitutional Au, since the diffusion profile is different [98]. For both spectra the values for $\hbar\omega$ and $\hbar\omega^*$ follow the systematic trend predicted by (11).

Our simple model yields rather consistent results for the different luminescent centers in Si. This suggests that in all cases it is the interstitial element which moves, that similar modes are excited during the optical transition and that the strength of the potential is predominantely scaled with the height of the diffusion barrier and only little affected by the partners in the complex. For very weak potentials (low H_m) and/or high complex stability the validity of the scaling rule is expected to break down and the defect binding energy becomes important.

6. Conclusion

In this paper we have summarized investigations on the various luminescence systems associated with 3*d* metals in Si. Not for all spectra the luminescent defects could be identified, but most probably all the centers are complexes containing two or more atoms. An exception may be V_i, but further investigations are needed for proof. The spectra can be divided into two classes. There are Fe and Cu related spectra which show the characteristics of exciton decay at isoelectronic centers, such as a high quantum efficiency, long exciton lifetimes and a spinless ground state of the luminescence transitions. On the other hand, Mn_4, CrB and CrGa play an important role for free-carrier recombination. The fine structures of the NP lines of their spectra reflect the occupation of the 3*d* shell of the TM in the centers and the low absolute intensities point to low quantum efficiencies of the transitions. Nevertheless concentrations of $5 \times 10^{12}\,cm^{-3}$ of the defects are detectable, e.g. for CrB independent of the B concentration up to $10^{18}\,cm^{-3}$. For the isoelectronic centers the observation of concentrations as low as $10^{10}\,cm^{-3}$ (e.g., Cu–Cu) cause no problem. Photoluminescence could thus be a very sensitive method to detect small concentrations of impurities in Si. The technique is a useful completion to DLTS or EPR, especially since isoelectronic centers are not detectable in EPR.

The optical transitions of all spectra (except V) take place between shallow effective mass like states 5 to 30 meV below the conduction band and the ground state of a donor or a pseudo-donor in the case of isoelectronic excitons. This allows it to correlate the optical data with electrical measurements. For CrB and CrGa there is an excellent agreement between optical ground state and electrical level position. On the other hand, for Mn_4, where the level positions are controverse in the literature, the luminescence has confirmed the midgap level position of the Mn_4 donor.

Calculations of 3*d*-level schemes by Watkins et al. [79] predict a ladder of TM states within the forbidden band gap. Optical transitions between such states should occur, but to date there are no luminescence lines which could be attributed to such intra *d*-shell transitions. We assume that the shallow initial states of the optical transitions near a band edge are efficient occupied by a cascade mechanism [100], whereas the capture time for free electrons in the deep internal states is rather long. In addition, there is a concurrence between radiative and nonradiative recombination mechanisms. In many cases the nonradiative path may dominate and quench the optical transition. This could also explain that other TM centers have not been observed in luminescence to date.

The spectra show rather low phonon coupling, therefore we conclude that there is only a small lattice relaxation between excited and ground state, and nonradiative multiphonon transitions have low probability. This is in agreement with investigations of excess carrier recombination in TM doped Si by Hangleiter [12, 13, 101]. To explain the experimental data, e.g. the temperature dependence of free-carrier lifetime, he excluded the possibility of effective multiphonon transitions but proposes an excitonic Auger mechanism. The phonon energies determined from the spectra follow a systematic trend, which also seems to be applicable to luminescent centers which contain other interstitial elements. The phonon energy seems to scale with the mass and the height of the diffusion barrier of the vibrating interstitial element.

Since luminescence studies of deep defects in Si are just at the beginning, further luminescent complexes containing 3*d* TM may be discovered in the future. It is well known that these impurities like to form pairs or more complicated complexes with many other impurities, e.g. Au [14, 38, 102] or S [103, 104]. Beyond TM very recently luminescence systems associated with the noble metals Au [96, 97, 105] or Pt [106–108] were reported and spectra of defects containing N and C [109, 110] identified. The growing number of deep luminescence systems discovered in Si in recent years makes photoluminescence a promising technique to study and identify deep defects even in Si – as the technique is frequently and successfully applied to study deep defects in III/V semiconductors.

Acknowledgements. The author wants to thank A. Hangleiter, R. Sauer, K. Thonke, and J. Weber for many stimulating discussions and valuable ideas. The encouragement and support by M. H. Pilkuhn is gratefully acknowledged. Thanks are due to H. Feichtinger, K. Graff, and E. R. Weber for constructive discussions and their help for center identifications by correlative measurements, to H. J. Queisser for a critical reading of the manuscript and to A. Axmann and G. Pensl for performing the ion implantations. The work was supported by the "Bundesministerium für Forschung und Technologie".

References

1. A. Rohatgi, J.R. Davies, R.H. Hopkins, P. Rai-Chondhury, P.G. McMullin, J.R. McCormick: Sol. State Electron. **23**, 415 (1980)
2. R.H. Hopkins, R.G. Seidensticker, J.R. Davies, P. Rai-Chondhury, P.D. Blais, J.R. McCormick: J. Crystl. Growth **42**, 493 (1977)
3. H. Lemke: Phys. Stat. Solidi (a) **64**, 215 (1981)
4. E.R. Weber: Appl. Phys. A **30**, 1 (1983)
5. K. Graff: Proc. 5th Intern. Symp. on Silicon Materials Science and Technology, Semiconductor Silicon (1986) ed. by H.R. Huff, T. Abe, B. Kolbesen, p. 751
6. A.G. Milnes: *Deep Impurities in Semiconductors* (Wiley, New York 1973)
7. J.W. Chen, A.G. Milnes: Ann. Rev. Mater. Sci. **10**, 157 (1980)
8. K. Graff, H. Pieper: J. Electrochem. Soc. **128**, 669 (1981)
9. H. Lemke: Phys. Stat. Solidi (a) **76**, 223 (1983)
10. K. Wünstel, P. Wagner: Appl. Phys. A **27**, 207 (1982)
11. H. Feichtinger: Acta Physica Austriaca **51**, 161 (1979)
12. A. Hangleiter: Proc. 13th Intern. Conf. on Defects in Semicond. (Coronado 1984) ed. by L.C. Kimerling and J.M. Parsey, Jr. (The Metallurgical Society of AIME, 1984) p. 213
13. A. Hangleiter, M.H. Pilkuhn: Proc. 17th Intern. Conf. on the Physics of Semiconductors (San Francisco 1984) ed. by J.D. Chadi, W.A. Harrison (Springer, New York 1984)
14. G.W. Ludwig, H.H. Woodbury: *Solid State Phys.* **13**, 223 (Academic, New York 1962)
15. H.H. Woodbury, G.W. Ludwig: Phys. Rev. **117**, 102 (1960)
16. H. Conzelmann, K. Graff, E.R. Weber: Appl. Phys. A **30**, 169 (1983)
17. P.J. Dean, C.H. Henry: Phys. Rev. **176**, 928 (1968)
18. P.J. Dean, M.S. Skolnick, Ch. Uihlein, D.C. Herbert: J. Phys. C **16**, 2017 (1983)
19. A couple of references are found in Physica **116** B, Chap. VI, Proc. 12th Intern. Conf. on Defects in Semiconductors (Amsterdam 1982) ed. by C.A.J. Ammerlaan
20. J.R. Haynes: Phys. Rev. Lett. **4**, 361 (1960)
21. For a review see P.J. Dean, D.C. Herbert: In *Excitons*, ed. by K. Cho, Topics Current Phys. **14**, (Springer, Berlin, Heidelberg 1979) p. 55
22. M.A. Vouk, E.C. Lightowlers: J. Lumin. **15**, 357 (1977)
23. M. Tajima: Appl. Phys. Lett. **32**, 719 (1978)
24. H. Nakayama, T. Nishino, Y. Hamakawa: Jpn. J. Appl. Phys. **19**, 501 (1980)
25. J. Weber, P. Wagner: J. Phys. Soc. Jpn. **49**, Suppl. A, 263 (1980), Proc. 15th Intern. Conf. on the Phys. of Semiconductors (Kyoto 1980), ed. by S. Tanaka and Y. Toyozawa
26. J. Weber, R. Sauer, P. Wagner: J. Lumin. **24/25**, 155 (1981)
27. J. Weber, H. Bauch, R. Sauer: Phys. Rev. B **25**, 7688 (1982)
28. S.P. Watkins, U.O. Ziemelis, M.L.W. Thewalt, R.R. Parsons: Solid State Commun. **43**, 687 (1982)
29. R. Sauer, J. Weber: Physica **116** B, 195 (1983), Proc. 12th Intern. Conf. on Defects in Semiconductors (Amsterdam 1982) ed. by C.A.J. Ammerlaan
30. H. Conzelmann, J. Weber: Physica **116** B (1983), Proc. 12th Intern. Conf. on Defects in Semiconductors (Amsterdam 1982) ed. by C.A.J. Ammerlaan, p. 291
31. H. Conzelmann: In 13th Intern. Conf. on Defects in Semiconductors (Coronado 1984) ed. by L.C. Kimerling and J.M. Parsey, Jr. The Metallurgical Society of AIME, p. 869
32. The ion implantations were done by A. Axmann, Institut für Angewandte Festkörperforschung, Freiburg, and G. Pensl, Universität Erlangen
33. K. Thonke, J. Weber, J. Wagner, R. Sauer: Physica **116** B, 252 (1983) Proc. 12th Intern. Conf. on Defects in Semiconductors (Amsterdam 1982), ed. by C.A.J. Ammerlaan
34. K. Thonke, G.D. Watkins, R. Sauer: Solid State Commun. **51**, 127 (1984)
35. L. Canham, G. Davies, E.C. Lightowlers: Physica **117** B, 119 (1983), Proc. 16th Intern. Conf. of Semiconductors, Part I (Montpellier 1982), ed. by M. Averous
36. R. Czaputa, H. Feichtinger, J. Oswald: Sol State Commun. **47**, 223 (1983)
37. H. Lemke: Phys. Stat. Solidi (a) **64**, 549 (1981)
38. H. Lemke: Phys. Stat. Solidi (a) **75**, 473 (1983)
39. K. Graff: Private communication
40. J. Hansen: Private communication
41. H. Conzelmann: Dissertation, U. Stuttgart (1985) unpublished
42. H. Feichtinger, R. Czaputa: Satellite Symp. to ESSDERC 82 (Munich 1982)
43. K.P. Abdurakhmanov, A.A. Lebedev, J. Kreissl, Sh.B. Utamuradova: Sov. Phys. Semicond. **19**, 133 (1985)
44. H. Feichtinger: Private communication
45. R.A. Faulkner: Phys. Rev. **184**, 713 (1969)
46. V.I. Fistul', V.M. Kazakova, Yu.A. Bobrovnikov, A.V. Ryabtsev, K.P. Abdurakhmanov, S. Zainabidinov, T.S. Kamilov, Sh.B. Utamuradova: Sov. Phys. Semicond. **16**, 603 (1982)
47. R.O. Carlson: Phys. Rev. **104**, 937 (1956)
48. G.W. Ludwig, H.H. Woodbury, R.O. Carlson: J. Phys. Chem. Solids **8**, 490 (1959)
49. M.M. Akhmedova, L.S. Berman, L.S. Kostina, A.A. Lebedev: Sov. Phys. Semicond. **9**, 1516 (1976)
50. A.O. Evwaraye: J. Appl. Phys. **48**, 3813 (1977)
51. M.L.W. Thewalt, U.O. Ziemelis, R.R. Parsons: Phys. Rev. B **24**, 3655 (1981)
52. M.L.W. Thewalt, U.O. Ziemelis, S.P. Watkins, R.R. Parsons: Can. J. Phys. **60**, 1691 (1982)
53. M.L.W. Thewalt, U.O. Ziemelis, R.R. Parsons: Solid State Commun. **39**, 27 (1981)
54. H. Conzelmann, A. Hangleiter, J. Weber: Phys. Stat. Solidi (b) **133**, 655 (1986)
55. S.P. Watkins, M.L.W. Thewalt, T. Steiner: Phys. Rev. B **29**, 5727 (1984)
56. S.P. Watkins, M.L.W. Thewalt: Can. J. Phys. **63**, 1074 (1985)
57. A. Chantre, D. Bois: Phys. Rev. B **31**, 7979 (1985)
58. T.E. Schlesinger, T.C. McGill: Phys. Rev. B **25**, 7850 (1982)
59. T.E. Schlesinger, T.C. McGill: Phys. Rev. B **28**, 3643 (1983)
60. T.E. Schlesinger, R.J. Hauenstein, R.M. Feenstra, T.C. McGill: Solid State Commun. **46**, 321 (1983)
61. H.D. Mohring, J. Weber, R. Sauer: Phys. Rev. B **30**, 894 (1984)
62. W. Bergholz: J. Phys. D **14**, 1099 (1981)
63. M.K. Bakhadyrkhanov, S. Zainoabidinov: Sov. Phys. Semicond. **12**, 398 (1978)
64. Y. Chikaura, K. Kishimoto: Jpn. J. Appl. Phys. **19**, L 5 (1980)
65. E. Scheibe, W. Schröter: Physica **116** B, 318 (1983), Proc. 12th Intern. Conf. on Defects in Semiconductors (Amsterdam 1982) ed. by C.A.J. Ammerlaan

66. W. Bergholz: Physica **116** B (1983), Proc. 12th Intern. Conf. on Defects in Semiconductors (Amsterdam 1982) ed. by C.A.J. Ammerlaan, p. 312
67. N.S. Minaev, A.V. Mudryi, V.D. Tkachev: Sov. Phys. Semicond. **13**, 233 (1979)
68. For a review, see P.J. Dean: J. Lumin. **7**, 51 (1973)
69. A. Baldereschi: J. Lumin. **7** (1973) p. 79 (theoretical)
70. J.J. Hopfield, D.G. Thomas, R.T. Lynch: Phys. Rev. Lett. **17**, 312 (1966)
71. J. Weber, W. Schmid, R. Sauer: Phys. Rev. B **21**, 2401 (1980)
72. P.J. Dean: Phys. Rev. B **4**, 2596 (1971)
73. W. Schmid: Phys. Stat. Solidi (b) **84**, 529 (1977)
74. S.A. Lyon, G.C. Osbourn, D.L. Smith, T.C. McGill: Solid State Commun. **23**, 425 (1977)
75. M.A. Vouk, E.C. Lightowlers: J. Lumin. **15**, 357 (1977)
76. T. Steiner, M.L.W. Thewalt: Solid State Commun. **49**, 1121 (1984)
77. G. Koster, J. Dimmock, R. Whealer, H. Statz: *Properties of the Thirty-Two-Point Groups* (MIT Press, Cambridge, MA 1963)
78. G.G. DeLeo, G.D. Watkins, W.B. Fowler: Phys. Rev. B **25**, 4972 (1982)
79. G.D. Watkins, G.G. DeLeo, W.B. Fowler: Physica **116** B, 28 (1983), Proc. 12th Intern. Conf. on Defects in Semiconductors (Amsterdam 1982), ed. by C.A.J. Ammerlaan
80. R. Sauer, J. Weber: Solid State Commun. **49**, 833 (1984)
81. J. Burgois, M. Lannoo: *Point Defects in Semiconductors* II, Springer Ser. Solid-State Sci. **35** (Springer, Berlin, Heidelberg 1983) Chap. 4 and 6
82. R. Sauer: Habilitation-Thesis (1978) unpublished
83. F. Beeler, O.K. Andersen, M. Scheffler: Phys. Rev. Lett. **55**, 1498 (1983)
84. F. Beeler, O.K. Andersen, M. Scheffler: Conf. Mat. Res. Soc., San Francisco (1985)
85. A.M. White: Solid State Commun. **32**, 205 (1979)
86. P. Vogl: Private communication
87. H. Feichtinger, J. Oswald, R. Czaputa, P. Vogl, K. Wünstel: 13th Intern. Conf. on Defects in Semiconductors (Coronado 1984) ed. by L.C. Kimerling and J.M. Parsey, Jr. (The Metallurgical Society of AIME) p. 115
88. A. Hangleiter, H. Conzelmann: Final Report T 85-162, Bundesministerium für Forschung und Technologie (1985)
89. W. Weber: Phys. Rev. B **15**, 4789 1(977)
90. G. Davies: Rep. Prog. Phys. **44**, 787 (1981)
91. M. Lannoo, J. Bourgois: *Point Defects in Semiconductors* I, Springer Ser. Solid-State Sci. **22** (Springer, Berlin, Heidelberg 1981) p. 219
92. R.C. Newman: *Infra-red Studies of Crystal Defects* (Taylor and Francis, London 1973)
93. D. Gilles, W. Bergholz, W. Schröter: J. Appl. Phys. **59**, 3590 (1986)
94. D. Senk, G. Borchardt: Mikrochim. Acta **2**, 477 (1983)
95. L. Canham, G. Davies, E.C. Lightowlers: J. Phys. C **13**, L 757 (1980)
96. J. Mazzaschi, J.C. Brabant, B. Brousseau, J. Barrau, M. Brousseau, F. Voillot: Solid State Commun. **39**, 1091 (1981)
97. D. Thebault, J. Barrau, M. Brousseau, DoXuan Thanh, J.C. Brabant, F. Voillot, Mme. Ribault: Solid State Commun. **45**, 645 (1983)
98. H. Conzelmann: To be published
99. W.R. Wilcox, T.J. LaChapelle: J. Appl. Phys. **35**, 240 (1964)
100. M. Lax: Phys. Rev. **119**, 1502 (1960)
101. A. Hangleiter: Phys. Rev. Lett. **55**, 2976 (1985)
102. M. Höhne: Phys. Stat. Solidi (b) **119**, K 117 (1983)
103. O.F. Schirmer: Physica **116** B, 306 (1983) 12th Intern. Conf. on Defects in Semiconductors (Amsterdam 1982) ed. by C.A.J. Ammerlaan
104. Sh.I. Askarov, M.K. Bakhadyrkhanov, V.F. Masterov, K.F. Shtel'makh: Sov. Phys. Semicond. **16**, 838 (1982)
105. D. Thebault, J. Barrau, G. Armelles, N. Lauret, J.P. Noguiev: Phys. Stat. Solidi (b) **125**, 357 (1984)
106. G. Armelles, J. Barrau, M. Brousseau, J.P. Noguier: Phys. Rev. B **33**, 1243 (1986)
107. G. Armelles, J. Barrau, M. Brousseau, J.P. Noguier: Solid State Commun. **56**, 205 (1985)
108. G. Armelles, J. Barrau, V. Thomas, M. Brousseau: J. Phys. C **19**, 2593 (1986)
109. A. Dörnen, G. Pensl, R. Sauer: Phys. Rev. B **33**, 1495 (1986)
110. A. Dörnen, G. Pensl, R. Sauer: Solid State Commun. **57**, 861 (1986)